

## Status and prospects for rare B decays at Belle II

---

**Elisa Manoni**<sup>a,\*</sup>

*<sup>a</sup>Istituto Nazionale di Fisica Nucleare, Sezione di Perugia  
Via Alessandro Pascoli, 23c, 06123 Perugia PG, Italia*

*E-mail: [elisa.manoni@pg.infn.it](mailto:elisa.manoni@pg.infn.it)*

In this talk we present recent results and prospects for New Physics searches in rare  $B$  decays at Belle II, focussing on the recent measurement of the  $B^+ \rightarrow K^+ \nu \bar{\nu}$  decay.

*Workshop Italiano sulla Fisica ad Alta Intensità (WIFAI2023)  
8-10 November 2023*

*Dipartimento di Architettura dell'Università Roma Tre, Rome, Italy*

---

\*Speaker

## 1. Rare $B$ decays and new physics searches at Belle II

Rare  $B$  meson decays are powerful probes for New Physics (NP). This may show up as new mediators (e.g. charged Higgs mediating the helicity- and CKM-suppressed  $B^+ \rightarrow \tau^+ \bar{\nu}$  decay) or as new final state particles (e.g. new sources of missing energy replacing the neutrinos in  $B^+ \rightarrow K^+ \nu \bar{\nu}$ ). In this contribution, Belle II measurements of  $B$  decays with missing energy or a photon in the final state will be discussed.

Searches of missing energy modes face the difficulties of having un-reconstructed particles in the final state. At B-factory experiments, this is mitigated by the fact that  $B$  mesons are produced in pairs, via  $e^+e^- \rightarrow \Upsilon(4S) \rightarrow B\bar{B}$  processes, and one of the  $B$  in the event ( $B_{\text{tag}}$ ) can be reconstructed in specific decay modes so that the accompanying  $B$  ( $B_{\text{sig}}$ ) properties can be inferred. Different tagging procedures are possible. In inclusive tagging analysis (ITA) the signal side particles are reconstructed and the property of the rest of the event (ROE) are exploited at background-rejection level; this corresponds to a 100% tagging efficiency since there is no explicit reconstruction of the  $B_{\text{tag}}$ . In order to have a higher purity sample, hadronic tagging analysis (HTA) can also be performed: in this case, the  $B_{\text{tag}}$  is reconstructed in a variety of hadronic final states through a multivariate approach [1], which results in a tagging efficiency at the per-cent level. The two methods can be adopted both in missing energy and radiative analyses.

## 2. Radiative $B$ decays

Belle II has a unique capability in studying  $b \rightarrow s\gamma$  and  $b \rightarrow d\gamma$ , both inclusively and using specific channels.

A search for the inclusive  $B \rightarrow X_s \gamma$  decay was performed using  $189 \text{ fb}^{-1}$  of data [2]. Such mode is sensitive to new physics [3] and the study of the photon energy spectrum allows to determine the b-quark mass and other non-perturbative parameters [4]. The experimental search is performed by reconstructing a high energy photon in the recoil of a hadronic  $B_{\text{tag}}$ . No constraints are imposed on the  $X_s$  system, to avoid hadronic uncertainties. The background suppression is based on the kinematic properties of the  $B_{\text{tag}}$ , properties of the signal side photon which allows to distinguish between candidates from  $B$  decays and asymmetric  $\eta$  and  $\pi^0$  decays, and event-shape variables which allow to reject  $e^+e^- \rightarrow q\bar{q}$  ( $q = u, d, s, c$ ) processes. The remaining background yield is determined from a fit to the  $B_{\text{tag}}$  beam-constrained mass ( $M_{\text{bc}}$ ) defined as  $M_{\text{bc}} = \sqrt{s/(4c^4) - p_B^*/c^2}$ , where  $s$  is the square of the energy of the colliding beams in the  $e^+e^-$  center-of-mass (c.m.) frame and  $p_B^*$  is the magnitude of the three-momentum of the  $B_{\text{tag}}$  in the c.m. system. The fit is performed in bins of the energy of the photon ( $E_\gamma^B$ ) in the  $B_{\text{sig}}$  rest frame, which is inferred from the  $B_{\text{tag}}$  kinematic properties. An example is given in the left plot of Fig. 1 for the  $1.8 < E_\gamma^B < 2.0 \text{ GeV}$  range. Non-signal decays are subtracted from data (an example is shown in the right plot of Fig. 1) and the branching fraction, in bins of  $E_\gamma^B$ , is measured (see Tab. 1). The results are consistent with the Standard Model (SM) expectation. Better (similar) statistical (systematic) precision, with respect to a BaBar analysis [5] on a sample of similar size, is achieved.

The full Belle dataset ( $711 \text{ fb}^{-1}$ ) and the Belle II sample ( $362 \text{ fb}^{-1}$ ), collected between 2019 and 2002 (Run 1), are used to measure branching fraction, CP asymmetry, and isospin asymmetry for the  $B \rightarrow \rho\gamma$  decay. The dominant background contribution is due to photon candidate from

$E_\gamma^B$ threshold [ GeV ]	$\mathcal{B}(B \rightarrow X_s \gamma)$ [ $10^{-4}$ ]
1.8	$3.54 \pm 0.78 \pm 0.83$
1.9	$3.06 \pm 0.56 \pm 0.47$
2.0	$2.49 \pm 0.46 \pm 0.35$

**Table 1:**  $B \rightarrow X_s \gamma$  analysis: integrated partial branching fractions for three  $E_\gamma^B$  thresholds. The first uncertainty is statistical and the second is systematic.

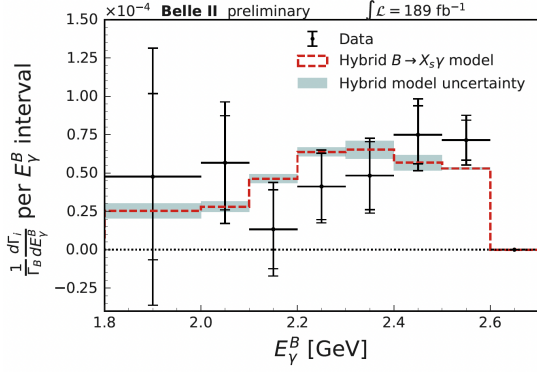
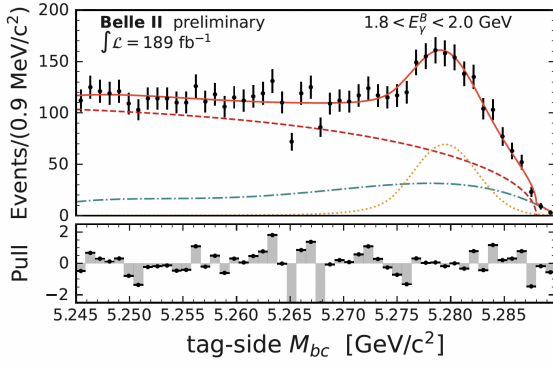


**Figure 1:** Left panel: distributions of (black markers with error bars)  $B_{\text{tag}} M_{bc}$  restricted to the  $1.8 < E_\gamma^B < 2.0$  GeV bin, with (curves) fit projections overlaid. The orange dotted curve corresponds to the correctly reconstructed  $B_{\text{tag}}$  from the generic  $B\bar{B}$  sample. The dashed and dash-dotted curves correspond to the  $q\bar{q}$  and misreconstructed  $B\bar{B}$  components. The solid red curve corresponds to the total fit. The pull distribution are shown in the bottom panel. Right panel: measured partial branching fractions  $(1/\Gamma_B)(d\Gamma_i/dE_\gamma^B)$  as a function of  $E_\gamma^B$ . The outer (inner) uncertainty bar shows the total (statistical) uncertainty. The overlaid model and uncertainty corresponds to the simulation of the signal events via an "hybrid model" [6].

asymmetric  $\eta$  and  $\pi^0$  decays and mis-reconstructed  $q\bar{q}$  final states, and a background suppression strategy similar to the one developed for the  $B \rightarrow X_s \gamma$  search is adopted. The signal yield is extracted from a simultaneous fit to the di-pion mass,  $M_{bc}$  computed for the  $\rho\gamma$  pair, and the difference between the expected and the observed  $B$  energy. The results of the analysis are given in Tab. 2. Those are the most precise measurements to date and the isospin asymmetry, which showed a  $2\sigma$  departure from null-asymmetry in the previous Belle analysis [10], is found to be consistent with zero.

### 3. Missing energy modes with $\tau$ 's in the final state

Purely leptonic  $B$  decays such as  $B^+ \rightarrow \tau^+ \nu$  are tree-level transitions, CKM- and helicity-suppressed in the SM. They are sensitive to NP models with heavy mediators and provide a complementary measurement of the CKM matrix element  $|V_{ub}|$  with respect to semileptonic  $b \rightarrow u\ell\nu$  final states. The SM predicts a branching fraction for  $B^+ \rightarrow \tau^+ \nu$  of the order of  $10^{-4}$ , with

Observable	Value
$\mathcal{B}(B^+ \rightarrow \rho^+ \gamma)$	$(13.1^{+2.0+1.3}_{-1.9-1.0}) \times 10^{-7}$
$\mathcal{B}(B^0 \rightarrow \rho^0 \gamma)$	$(7.5 \pm 1.3^{+1.0}_{-0.8}) \times 10^{-7}$
$A_{\text{CP}}(B^+ \rightarrow \rho^+ \gamma)$	$(-8.2 \pm 15.2^{+1.6}_{-1.2})\%$
$A_{\text{I}}(B \rightarrow \rho\gamma)$	$(10.9^{+11.2+6.8+3.8}_{-11.7-6.2-3.9})\%$

**Table 2:**  $B \rightarrow \rho\gamma$ : measured branching fractions, integrated CP asymmetry, and isospin asymmetry. The first uncertainty is statistical, the second is systematic, and the third for  $A_{\text{I}}$  is the uncertainty from  $f_{+-}/f_{00}$  [8] along with the lifetime ratio of  $B^+$  to  $B^0$  [7].

a precision ranging from 10 to 15% depending on the values used for the decay constant  $f_B$ , which parametrizes the  $b$ - $u$  annihilation process, and for  $|V_{ub}|$ . The world average of previous measurements, limited by statistical uncertainty, is  $\mathcal{B}(B^+ \rightarrow \tau^+ \nu) = (1.09 \pm 0.24) \times 10^{-4}$  [9]. Simulation studies performed by Belle II have been reported in Ref. [11]. Considering the HTA approach only, the precision will reach the 10% level with  $10 \text{ ab}^{-1}$  and with  $50 \text{ ab}^{-1}$  the measurement will be systematically limited, mainly due to the knowledge of the  $B_{\text{tag}}$  efficiency and of the modeling of backgrounds peaking in  $M_{bc}$  or containing  $K_L$  mesons. The precision will benefit from the usage of the semileptonic and inclusive tagging methods. The search for  $B^+ \rightarrow \tau^+ \nu$  on the Run 1 Belle II dataset is currently ongoing.

Several electroweak penguin modes with one or two  $\tau$ 's in the final state are also studied at Belle II. In the SM, the branching fraction for  $b \rightarrow s\tau\tau$  modes is predicted to be of the order of  $10^{-7}$ , with at 10% accuracy driven by form factor uncertainties [12]. Enhancements are possible in NP models in which couplings to the third generation of leptons are preferred [13]. Belle recently published a search for the  $B^0 \rightarrow K^{*0}\tau^+\tau^-$  [14] on the full Belle sample. No evidence for signal has been found and an upper limit on the branching fraction, at 90% confidence level, has been set at  $3.3 \times 10^{-3}$ . Simulation studies performed by Belle II have been reported in Ref. [11], considering the HTA approach in two different scenarios: a "baseline" scenario where, with respect to Belle, only the increase in the size of the data sample is considered, and an "improved" scenario where a 50% increase in signal efficiency for the same background level is assumed. In the former case the target integrated luminosity of  $50 \text{ ab}^{-1}$  will allow to set an upper limit of  $1.6 \times 10^{-3}$  while with the latter it will be possible to access the  $10^{-4}$  level with  $5 \text{ ab}^{-1}$ . Further improvements are foreseen by using semileptonic tag reconstruction and the addition of the charged final state. The search for  $B^0 \rightarrow K^{*0}\tau^+\tau^-$  on the Run 1 Belle II dataset is currently ongoing along with searches of other  $b \rightarrow s\tau^+\tau^-$  and  $b \rightarrow s\tau^+\ell^-$  modes.

#### 4. Search for $B^+ \rightarrow K^+ \nu \bar{\nu}$ decay

The SM branching fraction of the  $B^+ \rightarrow K^+ \nu \bar{\nu}$  decay is predicted to be  $\mathcal{B}(B^+ \rightarrow K^+ \nu \bar{\nu}) = (5.58 \pm 0.37) \times 10^{-6}$  [15] and can be significantly modified in models that predict non-SM particles [16]. In all analyses reported to date, no evidence for a signal has been found, and the current experimental upper limit on the branching fraction is  $1.6 \times 10^{-5}$  at the 90% confidence level [7].

Belle II performed a measurement [17] on the full Run 1 dataset combining the ITA and HTA methods, the first being more sensitive and the second more conventional. Except for the tagging method, the two analyses are kept as similar as possible and they select two almost statistically-independent samples.

Details on the ITA method, the driver for the final precision, and the results obtained by combining ITA and HTA will be given. Positive particle identification is requested for the signal kaon candidate, if more than one candidate per event is present the best one is chosen according to the smallest mass squared of the neutrino pair, defined as  $q_{\text{rec}}^2 = s/(4c^4) + M_K^2 - \sqrt{s}E_K^*/c^4$ , assuming the signal  $B$  meson to be at rest in the  $e^+e^-$  c.m. frame. Here  $M_K$  is the known mass of  $K^+$  mesons and  $E_K^*$  is the reconstructed energy of the kaon in the c.m. system. The background suppression is done by exploiting event shape, kinematics, vertexing, and missing energy information in two consecutive BDTs (BDT1 and BDT2). A sample-composition fit, in bins of the BDT2 output ( $\eta(\text{BDT2})$ ) and

$q_{\text{rec}}^2$  is used to extract the signal branching fraction relative to its SM expectation (signal strength  $\mu$ ). Dedicated studies, using a variety of control samples, are performed to validate the background description in simulated events. Where needed, correction factors are derived with corresponding systematic uncertainties. The backgrounds originating from  $B^0$  and  $B^+$  decays are dominant in the highest-sensitivity regions. The modeling of semileptonic  $B$  decays is checked in the BDT1 output signal region, while the simulation of hadronic  $B \rightarrow D^{(*)}K^+$  decays is validated in pion and lepton-enriched control samples. From a  $q_{\text{rec}}^2$  fit in the pion-enriched sample, a 1.3 scale factor to the size of  $B \rightarrow X_c (\rightarrow K_L X)$  contamination is derived. Another important class of background is charmless hadronic  $B$  decays with  $K_L$  mesons which can mimic the signal signature. In particular, correction on the modeling of the  $B^+ \rightarrow K^+ K_L K_L$  are derived by studying  $B^+ \rightarrow K^+ K_S K_S$ , where the explicit reconstruction of the final state particle is performed. The modeling of backgrounds from  $q\bar{q}$  events is checked on data taken 60 MeV below the  $\Upsilon(4S)$  resonance. The estimate of the signal efficiency is validated by using  $B^+ \rightarrow J/\Psi(\mu\mu)K^+$  control channel with an “embedding” procedure: the two muons from the  $J/\Psi$  are removed from the reconstructed objects to mimic the neutrinos and the signal kaon candidate is replaced with a signal kaon candidate from a simulated  $B^+ \rightarrow K^+ \nu\bar{\nu}$  event, to reflect the three-body topology of the signal signature. As a closure test of the ITA approach, the branching fraction for the  $B^+ \rightarrow \pi^+ K^0$  decay is measured by minimally adapting the ITA strategy. The result is found to be consistent with the world average. Several systematic uncertainties are considered, the dominant being from  $B\bar{B}$  background normalization, limited size of the simulated samples, and modeling of  $B^+ \rightarrow K^+ K_L K_L$  and  $B \rightarrow D^{**} \ell \nu$  decays. The data in the signal region of both ITA and HTA are shown in Fig. 2, with fit results overlaid. For HTA, the signal extraction variable is the output of the classifier used at the background-suppression stage ( $\eta(\text{BDTh})$ ). Good visual agreement between data and fit is observed in both samples. For the ITA, the signal strength is determined to be  $\mu = 5.4 \pm 1.0(\text{stat}) \pm 1.1(\text{syst})$ , corresponding to  $3.5 \sigma$  excess with respect to the background-only hypothesis and to  $2.9 \sigma$  deviation with respect to the SM expectation. For the HTA, the signal strength is determined to be  $\mu = 2.2^{+1.8}_{-1.7}(\text{stat})^{+1.6}_{-1.1}(\text{syst})$ , corresponding to  $1.1 \sigma$  excess with respect to the background-only hypothesis and to  $0.6 \sigma$  deviation with respect to the SM expectation. ITA and HTA results are in agreement at the  $1.2 \sigma$  level. The combined result for the signal strength yields  $\mu = 4.6 \pm 1.0(\text{stat}) \pm 0.9(\text{syst})$ , corresponding to a branching fraction of the  $B^+ \rightarrow K^+ \nu\bar{\nu}$  decay of  $[2.3 \pm 0.5(\text{stat})^{+0.5}_{-0.4}(\text{syst})] \times 10^{-5}$ . The significance with respect to the background-only hypothesis is found to be 3.5 standard deviations. This represents the first evidence for the  $B^+ \rightarrow K^+ \nu\bar{\nu}$  decay. The combined result is 2.7 standard deviations above the SM expectation. If compared with previous measurements [17], the ITA result is in agreement with previous hadronic-tag and inclusive measurements, while showing a  $2 \sigma$  tension with respect to measurements with semileptonic  $B$  tag. It has comparable precision with respect to previous best measurements. The HTA result is in agreement with all previous measurements and is the most precise result with hadronic tag method reported to date.

## References

- [1] T. Keck, *et al.*, *Comput. Softw. Big Sci.* **3** (2019) no.1, 6.
- [2] F. Abudinén *et al.* [Belle-II], [arXiv:2210.10220 [hep-ex]].

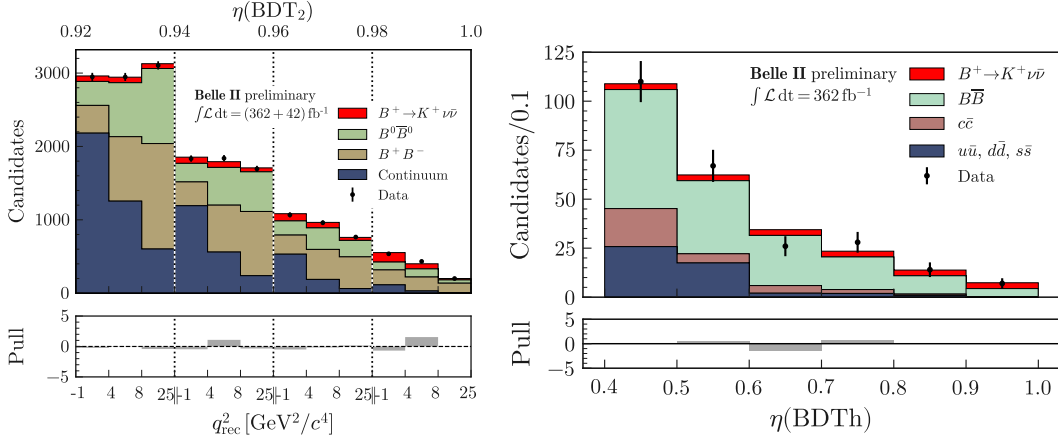


**Figure 2:** Observed yields and fit results in bins of the  $\eta(BDT2) \times q_{rec}^2$  space and of  $\eta(BDTh)$  as obtained by the ITA and HTA fits, respectively. In the former, the yields are shown individually for the  $B^+ \rightarrow K^+ \nu \bar{\nu}$  signal, neutral and charged  $B$ -meson decays and the sum of the five continuum categories, while in the latter  $B\bar{B}$  decays,  $c\bar{c}$  continuum, and light-quark continuum decays are included in the fit as background components. The pull distribution are shown in the bottom panel.

- [3] T. Hermann *et al.*, *JHEP* **11** (2012), 036.
- [4] F. U. Bernlochner *et al.* [SIMBA], *Phys. Rev. Lett.* **127** (2021) no.10, 102001.
- [5] B. Aubert *et al.* [BaBar], *Phys. Rev. D* **77** (2008), 051103.
- [6] C. Ramirez *et al.*, *Phys. Rev. D* **41** (1990), 1496.
- [7] R. L. Workman *et al.* [Particle Data Group], *PTEP* **2022** (2022), 083C01.
- [8] S. Choudhury *et al.* [Belle], *Phys. Rev. D* **107** (2023) no.3, L031102.
- [9] J. Lyon and R. Zwicky, *Phys. Rev. D* **88** (2013) no.9, 094004.
- [10] N. Taniguchi *et al.* [Belle], *Phys. Rev. Lett.* **101** (2008), 111801 [erratum: *Phys. Rev. Lett.* **101** (2008), 129904].
- [11] L. Aggarwal *et al.* [Belle-II], [arXiv:2207.06307 [hep-ex]].
- [12] J. L. Hewett, *Phys. Rev. D* **53** (1996), 4964-4969.
- [13] B. Capdevila *et al.*, *Phys. Rev. Lett.* **120** (2018) no.18, 181802.
- [14] T. V. Dong *et al.* [Belle], *Phys. Rev. D* **108** (2023) no.1, L011102.
- [15] W. G. Parrott *et al.* [HPQCD], *Phys. Rev. D* **107** (2023) no.1, 014511 [erratum: *Phys. Rev. D* **107** (2023) no.11, 119903].
- [16] D. Bečirević *et al.*, *Eur. Phys. J. C* **83** (2023) no.3, 252; J. Martin Camalich *et al.*, *Phys. Rev. D* **102** (2020) no.1, 015023; A. Filimonova *et al.*, *Phys. Rev. D* **101** (2020) no.9, 095006.
- [17] I. Adachi *et al.* [Belle-II], [arXiv:2311.14647 [hep-ex]].